Magnetic Fields in Galaxies

Rainer Beck

Max-Planck-Institut für Radioastronomie, Auf dem Hügel 69, 53121 Bonn,
Germany
`rbeck@mpifr-bonn.mpg.de`

1 Introduction

Magnetic fields are a major agent in the interstellar medium. They contribute significantly to the total pressure which balances the gas disk against gravitation. They affect the gas flows in spiral arms (Gómez and Cox, 2002). The effective sound speed of the gas is increased by the presence of strong fields which reduce the shock strength. The interstellar fields are closely connected to gas clouds. They affect the dynamics of the gas clouds (Elmegreen, 1981; de Avillez and Breitschwerdt, 2004). The stability and evolution of gas clouds are also influenced by magnetic fields, but it is not understood how (Crutcher, 1999; see Chap. 7). Magnetic fields are essential for the onset of star formation as they enable the removal of angular momentum from the protostellar cloud during its collapse (*magnetic braking*, Mouschovias, 1990). Strong fields may shift the stellar mass spectrum towards the more massive stars (Mestel, 1990). *MHD turbulence* distributes energy from supernova explosions within the ISM (Subramanian, 1998) and regenerates the field via *the dynamo process* (Wielebinski and Krause, 1993; Beck et al., 1996; Sect. 6). *Magnetic reconnection* is a possible heating source for the ISM and halo gas (Birk et al., 1998). Magnetic fields also control the density and distribution of cosmic rays in the ISM. A realistic model for any process in the ISM needs basic information about the magnetic field which has to be provided by observations.

Recent progress in observation of magnetic fields reveals the wide range of applications to large-scale MHD phenomena. Regular magnetic fields trace the gas flows in *barred galaxies* even if the gas can hardly be observed directly (Sect. 8). Regular fields can also help to feed their active galactic nuclei which may solve a long-standing problem. Vertical field lines above the disk of *edge-on galaxies* indicate strong galactic winds into a huge halo of hot gas, cosmic rays and magnetic fields (Sect. 9). *Interactions* between a galaxy and the intergalactic medium and between galaxies produce observable signatures in the magnetic field structure (Sect. 10). Finally, *jets* in spiral galaxies are rarely observed and spectacular (Sect. 11). Radio galaxies and their jets are discussed in Chap. 10.

2 Observing Extragalactic Magnetic Fields

Polarized emission at optical, infrared, submillimeter and radio wavelengths holds the clue to magnetic fields in galaxies. The only other method to detect magnetic fields is Zeeman splitting of spectral lines, which is restricted to observations of gas clouds in the Milky Way (Chap. 7).

Optical polarization is a result of extinction by elongated dust grains in the line of sight which are aligned in the interstellar magnetic field (the *Davis-Greenstein effect*). The **E**–vectors point parallel to the field. However, light can also be polarized by scattering, a process unrelated to magnetic fields and hence a contamination which is difficult to subtract (Fig. 1). Optical polarization surveys yielded the large-scale structure of the field in the local spiral arm of our Galaxy (Chaps. 5 and 7). The first extragalactic results by Hiltner (1958) were based on starlight polarization in M 31 and showed that the magnetic field is aligned along the galaxy's major axis. Appenzeller (1967) observed stars in several galaxies and found fields along the spiral arms. Significant progress was achieved by the group of Scarrott who detected polarization from diffuse light and could map the magnetic fields, e.g. in M 104 (Scarrott et al., 1997) and in M 51 (Scarrott et al., 1997). Figure 1 gives an example of more recent work.
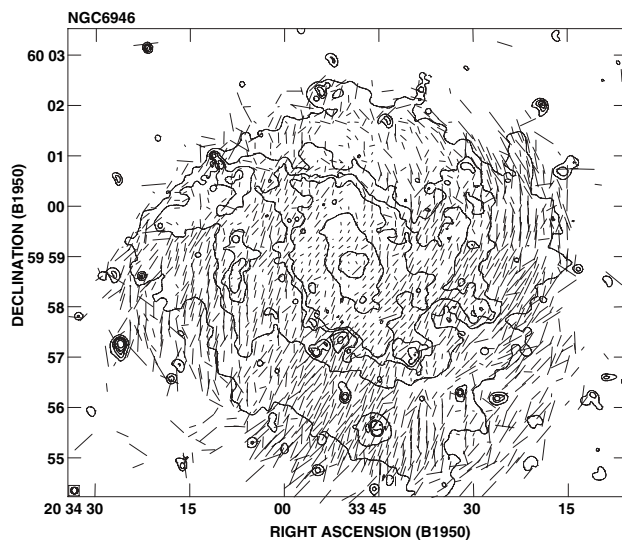
Fig. 1. Optical emission (contours) and polarization **E**–vectors of NGC 6946, observed with the polarimeter of the Landessternwarte Heidelberg at the MPIA Calar Alto 1-m telescope (Fendt et al., 1998). The polarization vectors are partly along the spiral arms (compare with radio **B**–vectors in Fig. 4). Polarization due to light scattering is obvious in the southern part

Polarization techniques in the infrared and submillimeter ranges, where emission from elongated dust grains is polarized and scattered light is no more a problem (Hildebrand, 1998; Chap. 7), are rapidly evolving (e.g. Greaves et al., 2000) and can be expected to contribute to our knowledge about interstellar magnetic fields in the near future.

In *radio continuum* the typical degrees of polarization are much higher than in the other spectral ranges, and we benefit from the development of large instruments and sensitive receivers. This is why most of our knowledge on interstellar magnetic fields in our Galaxy and in external galaxies is based on polarized radio emission and its Faraday rotation. A list of galaxies observed in polarization so far is given in Beck (2000).

The first detection of polarized radio emission in an external galaxy, M 51, came from Mathewson et al. (1972) using the then newly completed Westerbork Synthesis Radio Telescope, followed by Beck et al. (1978, 1980) who mapped the polarized

emission of M 31 with the Effelsberg telescope. The huge Effelsberg dish has been equipped with excellent receivers and polarimeters which made it especially successful in mapping magnetic fields and to detect weak diffuse emission (Figs. 7, 14, 15, 20, 24, 26). To achieve higher resolution, Effelsberg data are combined with interferometric (synthesis) data from the Very Large Array or the Australia Compact Array (Figs. 3–6, 4, 13, 16, 22). The first detection of polarized emission from external spiral galaxies with the VLA was reported in 1982 for M 51 (van der Hulst, Kennicutt and Crane, unpublished) and for NGC 4258 (van Albada and van der Hulst, 1982), and with the ATCA for NGC 1566 by Ehle et al. (1996).

Interstellar magnetic fields are illuminated by cosmic-ray electrons emitting *synchrotron radiation*, the dominant contribution to the diffuse radio continuum emission at centimeter and decimeter wavelengths. Synchrotron emission is intrinsically highly linearly polarized, 70–75% in a completely regular magnetic field. The observable degree of polarization in galaxies is reduced by the contribution of unpolarized thermal emission which may dominate in star-forming regions, by *Faraday depolarization* (increasing with wavelength) and by wavelength-independent depolarization by unresolved field structures within the telescope beam (Sokoloff et al., 1998).

A map of the *total intensity*, mostly of synchrotron origin, reveals the strength of the total interstellar magnetic fields in the plane of the sky, while the *polarized intensity and polarization angle* reveal the strength and structure of the regular fields in the plane of the sky which are resolved by the telescope beam.

The orientation of polarization vectors is turned in a magnetic plasma by *Faraday rotation* which is proportional to the line-of-sight integral over the density of thermal electrons multiplied by the strength of the regular field component along the line of sight. The sense of Faraday rotation gives the *direction* of the average regular field. At centimeter wavelengths the Faraday rotation angle ($\Delta\chi$) of the polarization vectors varies with λ^2. ($\Delta\chi = RM\,\lambda^2$, where RM is called the *rotation measure*.) Typical average interstellar rotation measures in mildly inclined galaxies are ±10–100 rad/m^2. This means that below about $\lambda3$ cm Faraday rotation is small and the **B**–vectors (i.e. the observed **E**–vectors rotated by $90°$) directly trace the *orientation* of the regular fields in the sky plane. Larger Faraday rotation is observed in edge-on galaxies, in the plane and near the center of the Milky Way (Chap. 5), in nuclear jets (Fig. 25), and in radio galaxies (up to several ±1000 rad/m^2).

Polarization angles are ambiguous by $\pm180°$ and hence insensitive to field reversals. Compression or stretching of turbulent fields generates incoherent anisotropic fields which reverse direction frequently within the telescope beam, so that Faraday rotation is small while the degree of polarization can still be high. On the other hand, strong Faraday rotation is a signature of *coherent regular fields* (Sect. 6).

3 Measuring Magnetic Field Strengths

Estimates of the dynamical importance of magnetic fields are based on their energy density which increases with the square of the field strength. Hence, the determination of field strengths is a primary task for observations. As the dynamical effects of magnetic fields are anisotropic due to their vector nature, the field structure is of similar importance (see Sect. 5).

The average strength of the total $\langle B_{t,\perp} \rangle$ and the resolved regular field $\langle B_{reg,\perp} \rangle$ in the plane of the sky can be derived from the total and polarized radio synchrotron intensity, respectively, if energy-density equipartition between cosmic rays and magnetic fields is assumed. The revised formula by Beck and Krause (2005), based on integrating the energy spectrum of the cosmic-ray protons, may lead to significantly different field strengths than the classical textbook formula which is based on integration over the radio frequency spectrum. Other sources of systematic bias are spectral steepening due to energy losses of the cosmic rays (Beck and Krause, 2005) and small-scale field fluctuations (Beck et al., 2003).

In our Galaxy the accuracy of the equipartition assumption can be tested, because we have independent information about the local cosmic-ray energy density from in-situ measurements and from γ-ray data. Combination with the radio synchrotron data yields a local strength of the total field $\langle B_t \rangle$ of $6\,\mu G$ and about $10\,\mu G$ in the inner Galaxy (Strong et al., 2000), similar values as derived from energy equipartition (Berkhuijsen, in Beck, 2001).

The field strength is determined by the mean surface brightness (intensity) of radio synchrotron emission and thus does not depend on the size of a galaxy. The mean equipartition strength of the total field for a sample of 74 spiral galaxies (Niklas, 1995) is $\langle B_t \rangle \simeq 9\,\mu G$. Dwarf galaxies may host fields of similar strength as spirals if their star-formation rate is high enough (Sect. 7). On the other hand, giant spirals with weak star-forming activity and low radio surface brightness like M 31 (Fig. 7) have $\langle B_t \rangle \simeq 6\,\mu G$. In grand-design galaxies with massive star formation like M 51 (Fig. 3), M 83 (Fig. 6) and NGC 6946 (Fig. 4) $\simeq 15\,\mu G$ is a typical average strength of the total field. In the prominent spiral arms of M 51 the total field strength is 25–30 μG (Fletcher et al., 2004b). Field compression by external forces like interaction may also lead to very strong fields (Sect. 10). The strongest fields in spiral galaxies were found in starburst galaxies like M 82 with $\simeq 50\,\mu G$ strength (Klein et al., 1998), the 'Antennae' (Fig. 22), in nuclear rings like in NGC 1097 (Fig. 19) and NGC 7552 with $\simeq 100\,\mu G$ strength (Beck et al., 2004), and in nuclear jets (Fig. 25). If energy losses of electrons are significant in starburst regions or massive spiral arms, these values are lower limits (Beck and Krause, 2005).

The strength of resolved regular fields B_{reg} in spiral galaxies (observed with spatial resolutions of a few 100 pc) is typically 1–5 μG. Exceptionally strong regular fields are detected in the interarm regions of NGC 6946 of $\simeq 13\,\mu G$ (Beck and Hoernes, 1996; Fig. 4) and $\simeq 15\,\mu G$ at the inner edge of the inner spiral arms in M 51 (Fletcher et al., 2004b; Fig. 5). In spiral arms of external galaxies the resolved regular field is generally weaker and the tangled (unresolved) field is stronger due to turbulent gas motion in star-forming regions and the expansion of supernova remnants. In interarm regions the regular field is generally stronger than the tangled field.

The relative importance of various competing forces in the interstellar medium can be estimated by comparing the corresponding energy densities. In the local Milky Way, the energy densities of the stellar radiation field, turbulent gas motions, cosmic rays, and magnetic fields are similar (Boulares and Cox, 1990). A global study was performed in the spiral galaxy NGC 6946 (Fig. 2). The energy density of the warm ionized gas E_{th} in NGC 6946 is one order of magnitude smaller than that of the total magnetic field E_{magn}, i.e. the ISM is a low-β plasma ($\beta = E_{th}/E_{magn}$),

ENERGY DENSITIES IN NGC6946
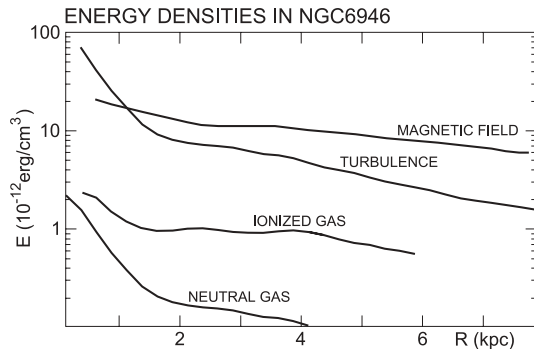
Fig. 2. Radial variation of the energy densities of the total magnetic field, turbulent motion of the neutral gas, thermal energy of the ionized gas, and thermal energy of the neutral gas in NGC 6946 – determined from observations of non-thermal and thermal radio continuum, and CO and HI line emission (Beck, 2004)

similar to the Milky Way (Boulares and Cox, 1990). The contribution of hot gas, which may increase β, is probably small (Ehle et al., 1998).

In the inner parts of NGC 6946 the energy densities of the total magnetic field and turbulent gas motion are similar, an argument for a close connection between field and gas clouds (see Sect. 4). The field dominates in the outer parts due to the large radial scale length of the total field B_t ($l_t \simeq 16$ kpc), compared to the scale length l_ρ of about 3 kpc for the neutral density ρ. This is in conflict with the models of turbulent generation of interstellar magnetic fields which predict similar scale lengths for B_{turb}^2 and ρ. As the degree of polarization (and hence the field regularity) increases with increasing radius, the total field in the outer regions of galaxies becomes dominated by the regular field, so that the scale length of B_{turb} is smaller than that of B_t, but not small enough to match l_ρ.

The field in the outer region of galaxies may be amplified by a dynamo driven by the *magneto-rotational instability (MRI*; Sellwood and Balbus, 1999; Rüdiger and Hollerbach, 2004) which is believed to drive turbulent gas motion outside the star formation regime. MRI can generate magnetic energy densities beyond that of turbulent motions. Detailed models are being developed.

In the outermost parts of spiral galaxies the magnetic field energy density may even reach the level of global rotational gas motion and affect the rotation curve, as proposed by Battaner and Florido (2000). Field strengths in the outer parts of galaxies can be measured by Faraday rotation of polarized background sources. Han et al. (1997) found evidence for regular fields in M 31 out to 25 kpc radius (Sect. 6).

4 Magnetic Fields and Gas Clouds

Strongest total radio emission (i.e. total magnetic fields) generally coincide with highest emission from dust and cool gas in the spiral arms. Comparison of the maps of the total radio emission of M 51 and the mid-infrared dust emission at $\lambda 7$ μm and $\lambda 15$ μm (Sauvage et al., 1996) reveals a surprisingly close connection (Fig. 3). In NGC 6946, the highest correlation of all spectral ranges is between the total radio emission at $\lambda 6$ cm and the mid-infrared dust emission, while the correlation with the cold gas (as traced by the CO(1-0) transition) is less tight (Frick et al., 2001; Walsh et al., 2002).
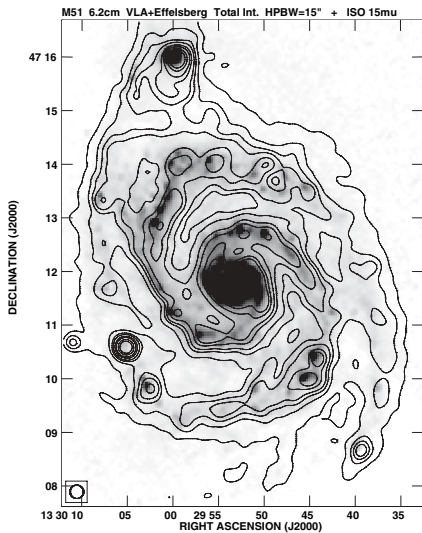
Fig. 3. Total radio continuum emission of M 51 at $\lambda 6$ cm with $15''$ beam size (contours), combined from Effelsberg and VLA observations (Fletcher et al., 2004b). The background image shows the $\lambda 15\,\mu$m infrared emission from observations of the ISO satellite (Sauvage et al., 1996)
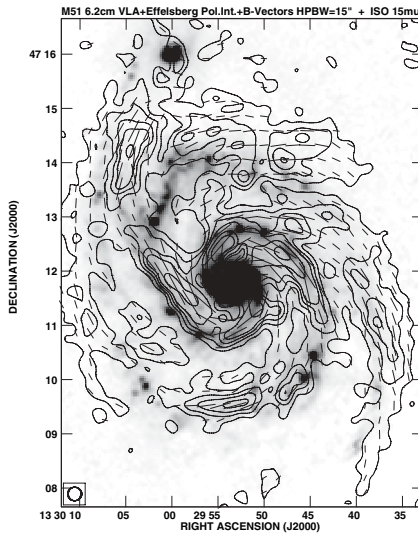
Fig. 4. Polarized radio emission (contours) and B–vectors of M 51 at $\lambda 6$ cm, combined from Effelsberg and VLA observations (Fletcher et al., 2004b). The background image shows the $\lambda 15\,\mu$m infrared emission (Sauvage et al., 1996)

The physical background of the relation is hardly understood. Energetic photons from massive stars cause infrared and thermal radio emission. However, over most of the observable radio frequency range the emission is dominated by the nonthermal synchrotron process. Magnetic fields and star-formation processes must be connected. Probably the fields are coupled to the dense, mostly neutral *gas clouds*, which are mixed with the dust. The density of the hot gas is too low to contribute significantly to the anchoring of field lines in the galaxy disks. Niklas and Beck (1997) and Hoernes et al. (1998) proposed a scaling $B_{\rm t} \propto \rho^{1/2}$ where ρ is the average density of the neutral (atomic + molecular) within the telescope beam, similar to the scaling in dense molecular clouds (Chap. 7). As the volume filling factor of the clouds is low, ρ mainly depends on the average *number density* of clouds within the volume observed by the beam, not on their internal density. In this case, the above scaling can be interpreted as magnetic flux freezing in the compressible 'fluid' of gas clouds. The total field strength $B_{\rm t}$ is highest in spiral arms where the number density of clouds is highest. This number may control the star-formation rate and the magnetic flux.

Photoionization may provide sufficient density of thermal electrons in the outer regions of gas clouds to hold the field lines, as indicated by C^+ emission from the warm surfaces of molecular clouds (Stacey et al., 1991). A Faraday screen of ionized gas has been detected in front of the Taurus molecular cloud complex in our

Galaxy (Wolleben and Reich, 2004). Polarization observations in the submillimeter range also indicate strong and distorted fields in the surroundings of molecular/dust clouds (Greaves et al., 1994).

5 Magnetic Field Structure

Radio *polarization* observations show that in most galaxies the regular field follows the spiral structure seen in the stars and the gas, e.g. in M 51 (Neininger, 1992; Neininger and Horellou, 1996; Fig. 4 and 5), M 81 (Krause et al., 1989b; Fig. 8), and M 83 (Neininger et al., 1991; Fig. 6), though the regions of strongest regular fields are generally *offset* from the spiral arms (see below). As the motion of gas and stars is not along the spiral density wave, but crosses the spiral arm, the magnetic field pattern does *not* follow the gas flow. If large-scale magnetic fields were frozen into the gas, differential rotation would have wound them up to very small pitch angles. The large observed pitch angles ($10°$–$40°$) indicate decoupling between gas and magnetic fields due to magnetic diffusivity which is essential for dynamo action (Sect. 6).
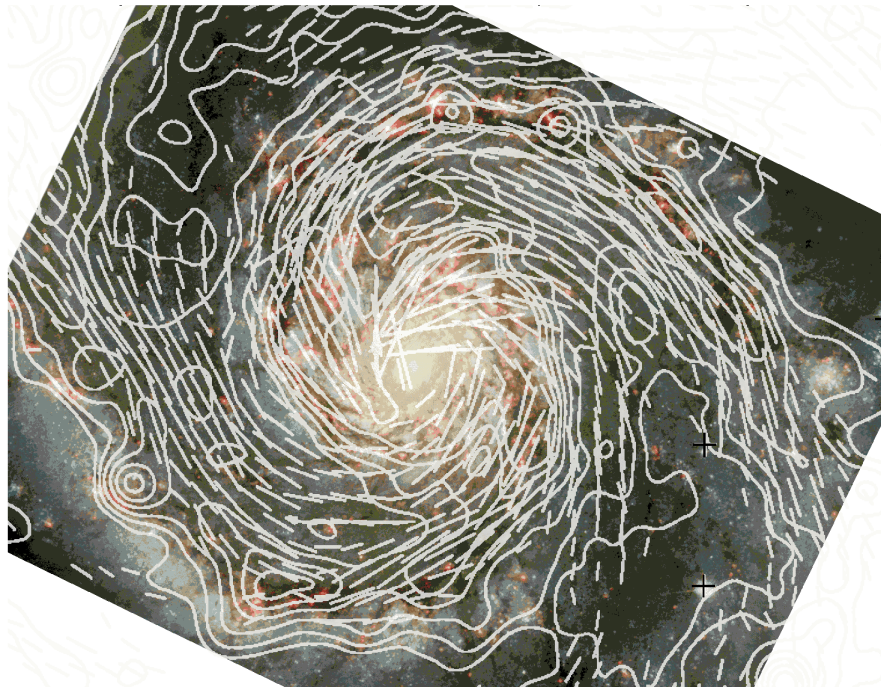
Fig. 5. Total radio emission (contours) and B–vectors from the inner disk of M 51 at $\lambda 6$ cm, combined from VLA and Effelsberg observations (Fletcher et al., 2004b). The field size is $4' \times 3'$, the beam size $6''$. The background image shows the optical emission observed with the Hubble Space Telescope (Hubble Heritage Project)
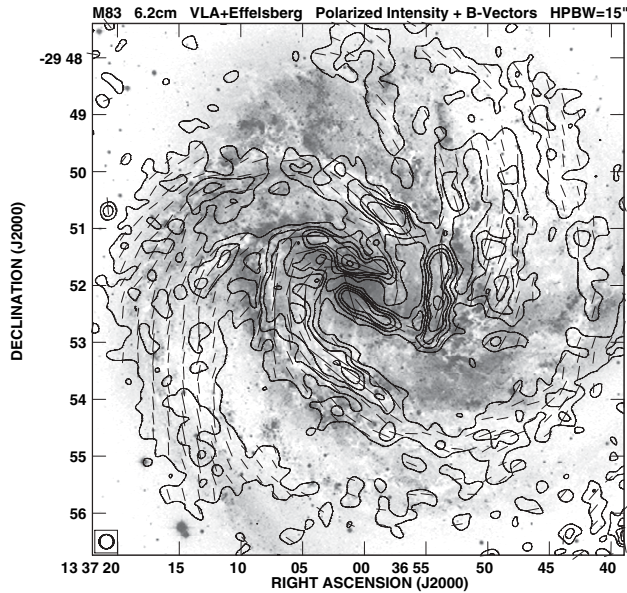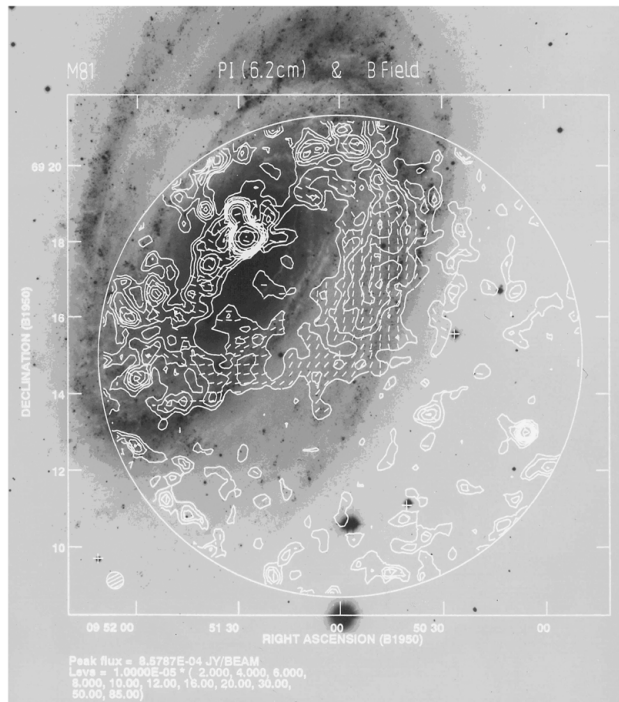
Fig. 6. Polarized radio emission (contours) and B–vectors of M 83 at $\lambda6$ cm with $15''$ beam size, combined from VLA and Effelsberg observations (Beck, Ehle and Sukumar, unpublished); the background optical image is from the Anglo Australian Observatory (Malin, priv. comm.)
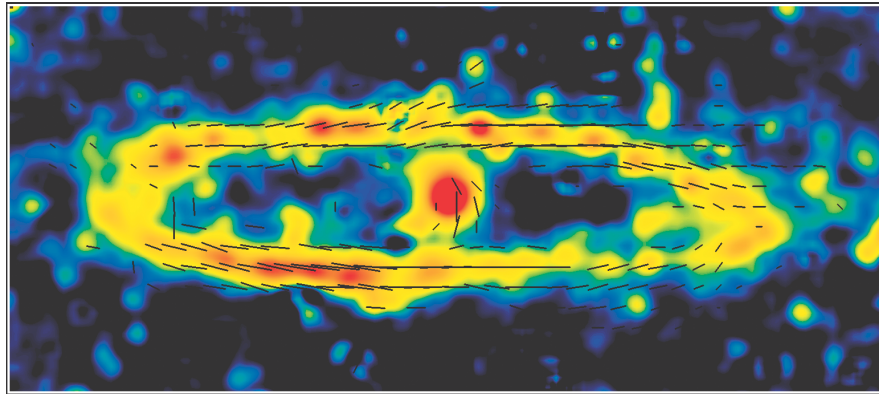
Fig. 7. Total radio emission (contours) and B–vectors (corrected for Faraday rotation) of M 31 at $\lambda6$ cm, observed with the Effelsberg telescope (Berkhuijsen et al., 2003). The field size is $130' \times 57'$, the beam size $3'$

In the spiral arms, polarized emission is generally weak, because the regular field is unresolved in the spiral arms due to field tangling by increased turbulent motions of gas clouds or by supernova shock fronts, and, at longer wavelengths, due to Faraday depolarization (Sokoloff et al., 1998). Turbulent fields, as indicated by unpolarized emission, are generally enhanced in spiral arms, following the general scaling with gas density (Sect. 4).
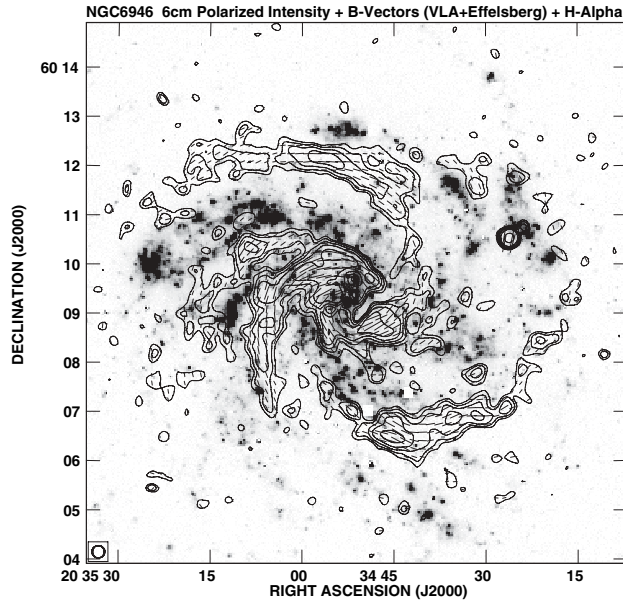
Fig. 8. Polarized radio emission (contours) and B–vectors of M 81 at $\lambda 6$ cm with $25''$ beam size, observed with the VLA (Schoofs, 1992). The circle shows the radius of the primary beam at the 25% intensity level. The intensities are corrected for primary-beam attenuation

In galaxies with strong density waves like M 51 three components of the regular field can be distinguished (Fig. 5). One component fills the interarm space, like in NGC 6946 (Fig. 4). The second component is strongest at the positions of the prominent dust lanes on the inner edge of the gaseous spiral arms, as expected from field alignment by compression. However, the arm-interarm contrast is low, which is in conflict with classical shock compression models and calls for new models of spiral arm formation (e.g Gómez and Cox, 2002). The third component of regular field coincides with the outer southern and southwestern spiral arms, without signs of compression (Fig. 4).

M 83 (Fig. 6) and NGC 2997 (Han et al., 1999) are cases similar to M 51, with enhanced regular fields at the inner edges of the inner optical arms, regular fields in some interarm regions, and also regular fields coinciding with the outer optical arms.

In the highly inclined galaxy M 31 (Fig. 7) the spiral arms are hard to distinguish. Star formation activity is restricted to a limited radial range around 10 kpc radius (the 'ring'). The strongest regular fields coincide with massive dust lanes, but regular fields were detected out to 25 kpc radius (Han et al., 1998). Other density-wave galaxies like M 81 (Krause et al., 1989b; Fig. 8) and NGC 1566 (Ehle et al., 1996) show little signs of field compression; regular fields occur mainly in *interarm regions.*

Observations of another gas-rich galaxy, NGC 6946, revealed a surprisingly regular distribution of polarized emission with two symmetric *magnetic arms* located in interarm regions, without any association with observable gas or stars, and running

NGC6946 6cm Polarized Intensity + B-Vectors (VLA+Effelsberg) + H-Alpha

Fig. 9. Polarized radio emission (contours) and B–vectors of NGC 6946 at $\lambda 6\,\mathrm{cm}$ with $15''$ beam size, combined from VLA and Effelsberg observations (Beck and Hoernes, 1996). The background image shows the Hα emission (Ferguson et al., 1998)

NGC6946 20.5cm VLA Polarized Intensity HPBW=15"
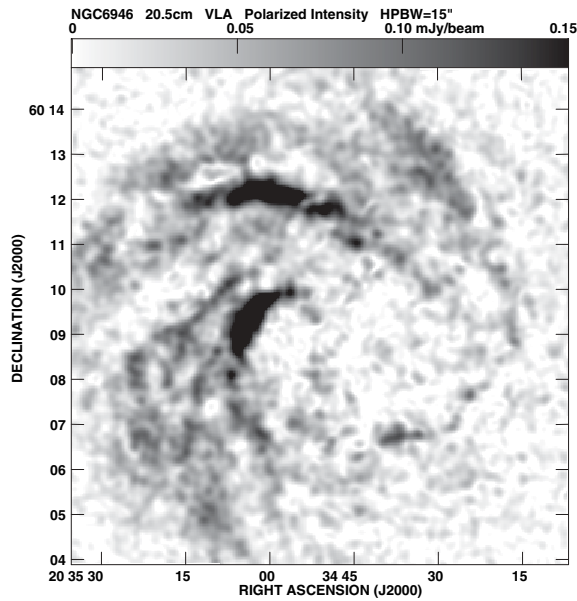
Fig. 10. Polarized radio emission of NGC 6946 at $\lambda 20\,\mathrm{cm}$, combined from VLA C- and D-array observations. The field is the same as in Fig. 4, the beam size is $15''$ (Beck, unpublished)

parallel to the adjacent optical spiral arms (Fig. 4). These magnetic arms do not fill the entire interarm spaces like the polarized emission in M81, but are less than 1 kpc wide. Their degree of polarization is exceptionally high (up to 50%); the field is *almost totally aligned*. With the higher sensitivity at $\lambda 20\,\mathrm{cm}$ (Fig. 10), more

IC342 20.5cm VLA Polarized Intensity HPBW=30"
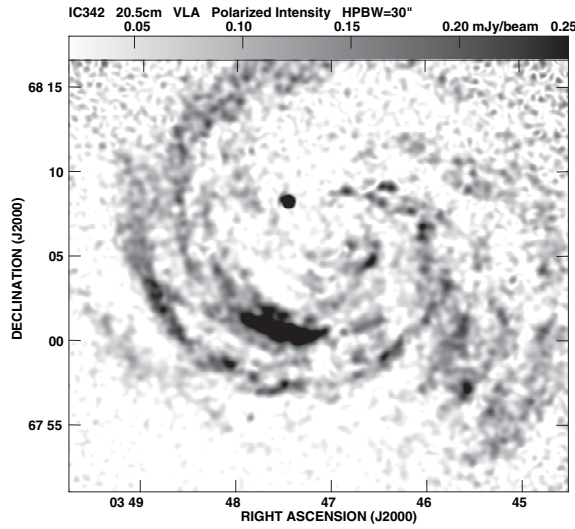
Fig. 11. Polarized radio emission of IC 342 at $\lambda20\,$cm, combined from VLA C- and D-array observations. The field size is $32' \times 32'$, the beam size $30''$ (Beck, unpublished)

NGC 2442 5.8cm ATCA Total Intensity + B-vectors HPBW=10"
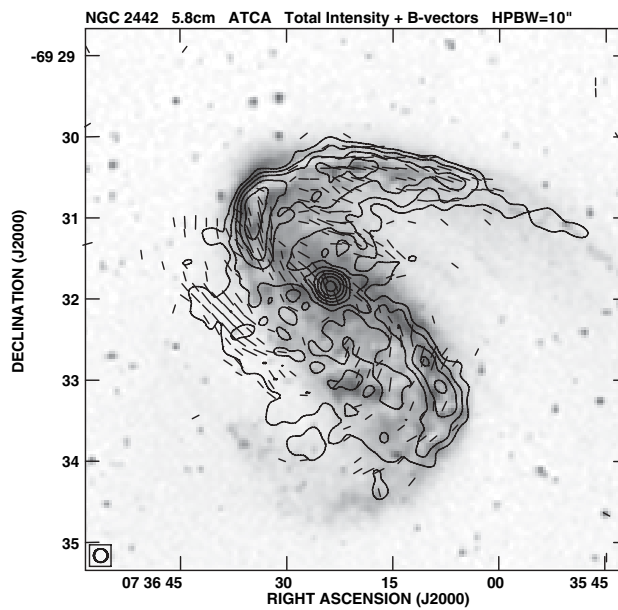
Fig. 12. Total radio emission (contours) and B–vectors of NGC 2442 at $\lambda6\,$cm with $10''$ beam size, observed with the ATCA (Harnett et al., 2004). The background image shows the Hα emission, smoothed to the same resolution

magnetic arms appear in the northern half of NGC 6946, extending far beyond the optical arms, while the strong Faraday depolarization at this wavelength hides the southern magnetic arm. Magnetic arms outside of the optical arms have also been found in M 83 (Fig. 6), in NGC 2997 (Han et al., 1999), and in NGC 2442 (Fig. 12).

Several models have been proposed to explain the generation of magnetic arms. Fan and Lou (1997) suggested that they could be manifestations of slow MHD waves which may propagate in a rigidly rotating disk, with the maxima in field strength

phase-shifted against those in gas density. However, all galaxies with magnetic arms rotate differentially beyond 1–2 kpc from the center. Differential rotation destabilizes slow waves so that they evolve into Parker instabilities, so that dynamo models are more promising to explain the magnetic arms (Chap. 6).

Regular magnetic fields form spiral patterns which can also be disconnected from the optical spiral arms. Long, highly polarized arms were first discovered in the outer regions of IC 342 where only faint arms of HI radio line emission exist (Krause et al., 1989a; Krause, 1993). More recent observations at $\lambda 20$ cm revealed a system of such features (Fig. 11; note that the inner part of IC 342 is Faraday-depolarized at this wavelength).

External forces may also compress the magnetic field. In NGC 2442 (Harnett et al., 2004) and in the Virgo cluster member NGC 4254 (Soida et al., 1996) the polarized emission on one side of the galaxy is shifted towards the *outer* edge of the spiral arm, an indication for ram pressure by the intracluster medium. In NGC 3627 (Fig. 13), member of the Leo triplett, the magnetic arm and the optical arm are totally misaligned on the eastern side, another sign of interaction (see Sect. 10).
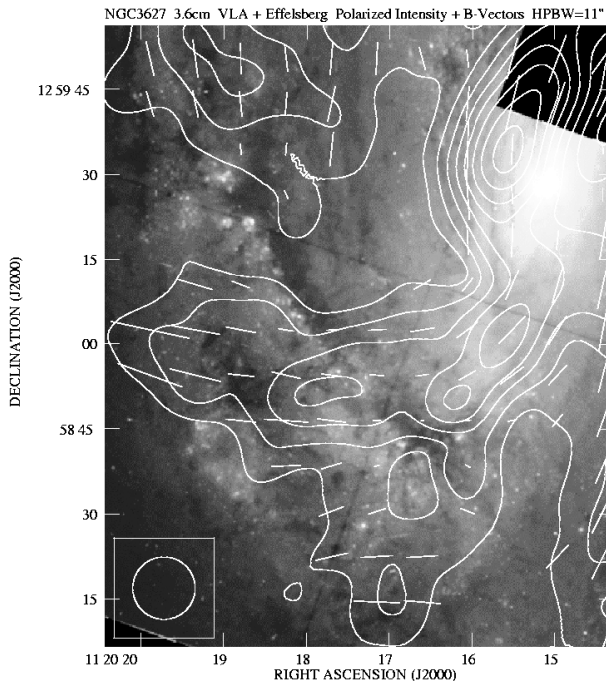
Fig. 13. Polarized radio emission (contours) and B–vectors of NGC 3627 at $\lambda 3.6$ cm with $11''$ beam size, combined from VLA and Effelsberg observations (Soida et al., 2001). The background optical image is from the Hubble Space Telescope

Large-scale *field reversals* were discovered in the Milky Way (Chaps. 5 and 6), but nothing similar has yet been detected in spiral galaxies. High-resolution maps of Faraday rotation, which measure the RMs of the diffuse polarized synchrotron emission and are sensitive to reversals, are available for a couple of spiral galaxies. In M 81 the dominating bisymmetric field structure implies two large-scale reversals (Krause et al., 1989b). The disk fields of M 51 and NGC 4414 can be described by

a mixture of dynamo modes where reversals may emerge in a limited radial and azimuthal range of the disk (Berkhuijsen et al., 1997; Soida et al., 2002; Chap. 6). However, no multiple reversals along radius, like those in the Milky Way, were found so far in the disk of any external galaxy.

The discrepancy between Galactic and extragalactic data may be due to the different volumes traced by the observations. Results in the Galaxy are based on pulsar RMs which trace the warm ionized medium near the plane, while extragalactic RMs of the diffuse polarization emission are averages over the line of sight through the whole thick disk or the halo. Furthermore, some of the Galactic reversals may be due to local field distortions or loops (Mitra et al., 2003). RM data at high frequencies are needed to obtain a clear picture of the field structure in the Milky Way.

Present-day polarization observations cannot resolve the detailed field structure, especially in the spiral arms where the degrees of polarization are low due to beam smearing. Rotation measure data from Galactic pulsars (Chap. 5) and depolarization data in external galaxies (Beck et al., 1999b) indicate that the interstellar field is turbulent on scales of $\simeq 20$ pc. The highest spatial resolutions obtained so far are $\simeq 50$ pc in M 31 (Hoernes, 1997) and $\simeq 100$ pc in IC 342 (Beck, in prep.). The new ATCA polarization survey of the Magellanic Clouds has about 10 pc resolution (Gaensler et al., 2005).

6 Dynamos

Observation of large-scale patterns in Faraday rotation measures, e.g. in M 31 (Berkhuijsen et al., 2003; Fletcher et al., 2004a; Fig. 14), NGC 6946 (Beck, 2001) and NGC 2997 (Han et al., 1999), shows that the regular field in these galaxies has a coherent direction and hence is not generated by compression or stretching of irregular fields in gas flows.

Coherent primordial fields, if they existed, are hard to be preserved over a galaxy's lifetime (see however Chap. 4). The dynamo mechanism (Chap. 6) is able to generate and preserve coherent magnetic fields, and these are of appropriate spiral shape (Beck, 1993; Beck et al., 1996). However, the pitch angle of the field spiral depends on the dynamo number, *not* on the pitch angle of the gaseous spiral (Rohde et al., 1999). The observed alignment of magnetic pitch angles with those of the gaseous arms can be achieved by inclusion of the shear flow around spiral arms (Linden et al., 1998; Elstner et al., 2000). The dynamo needs some seed field to start operation. The seed field can be turbulent, e.g. ejected from supernovae or stellar winds (Chap. 1) or from early starbursts (Chap. 2), or a primordial field (Chap. 4).

The field structure obtained in *mean-field α–Ω dynamo models* is described by modes of different azimuthal and vertical symmetry. The existing dynamo models (Beck et al., 1996) predict that several azimuthal modes can be excited, the strongest being $m = 0$ (an axisymmetric spiral field), followed by the weaker $m = 1$ (a bisymmetric spiral field), etc. These generate a Fourier spectrum of azimuthal RM patterns. The axisymmetric mode with even vertical symmetry (quadrupole) is excited most easily. For most of about 20 nearby galaxies observed so far, the RM data indicate a mixture of magnetic modes which cannot be reliably determined due to low angular resolution and/or low signal-to-noise ratios (Beck, 2000).
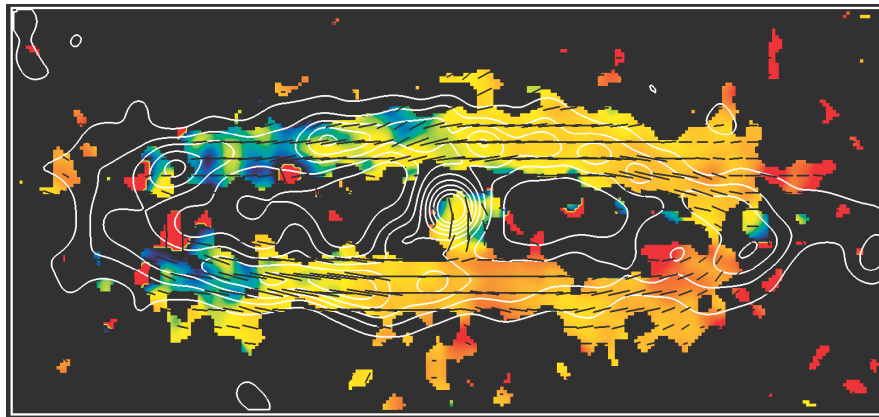
Fig. 14. Total radio emission of M 31 at $\lambda6\,\mathrm{cm}$ (contours) and Faraday rotation measures between $\lambda6\,\mathrm{cm}$ and $\lambda11\,\mathrm{cm}$, observed with the Effelsberg telescope. The field size is $130'$ x $57'$, the beam size $5'$ (Berkhuijsen et al., 2003)

M 31 is an exception with a strongly dominating axisymmetric field (Beck, 1982; Berkhuijsen et al., 2003; Fig. 14). This field structure extends to at least 25 kpc radius (Han et al., 1998) and at least 1 kpc height above the galaxy's plane (Fletcher et al., 2004a). A bisymmetric mode dominates in M 81 (Krause et al., 1989b).

Magnetic arms (Sect. 5) can be understood to evolve between the optical arms if the dynamo number is smaller in the gaseous arms than between them, e.g. due to increased turbulent velocity of the gas in the arms (Moss, 1998; Shukurov, 1998; Chap. 6) or if turbulent diffusion is larger in the arms (Rohde et al., 1999); the magnetic arms in NGC 6946 are a superposition of an axisymmetric $m = 0$ and a quadrisymmetric $m = 2$ mode.

Spiral fields can be traced to within a few 100 pc from the centers of M 51 (Fig. 5), NGC 2997 (Han et al., 1999) and NGC 6946 (Fig. 4). Mean-field dynamo models can hardly reproduce this result because differential rotation is too weak near the centers of these galaxies. Enhancement of velocity shear by strong density waves (e.g. in M 51) or a non-axisymmetric gas flow around a nuclear bar (e.g. in NGC 6946) or inflow by magnetic stress (Sect. 8) are needed to increase dynamo action.

The strong fields in the outer regions of galaxies (Fig. 2) require non-standard dynamos in regions with low star formation. The *magneto-rotational instability* (MRI) transfers energy from the shear of differential rotation into turbulent and magnetic energy (Sellwood and Balbus, 1999; Rüdiger and Hollerbach, 2004). Other non-standard dynamos, which are faster than the mean-field α–Ω dynamo, have been proposed for young galaxies, e.g. driven by a *cross-helicity correlation* between the small-scale components of gas velocity and magnetic field (Brandenburg and Urpin, 1998), or by cosmic rays inflating buoyant *Parker loops* (Parker, 1992; Moss et al., 1999; Hanasz and Lesch, 2000; Hanasz et al., 2002).

Observation of a large sample of galaxies at medium and large distances with next-generation radio telescopes like the Square Kilometer Array will provide the data base to test dynamo against primordial theory (Beck and Gaensler, 2004).

# 7 Magnetic Fields in Flocculent and Irregular Galaxies

Regular magnetic fields with strengths similar to those in grand-design spiral galaxies have been detected in the flocculent galaxies M 33 (Buczilowski and Beck, 1991, Fig. 15), NGC 3521 and NGC 5055 (Knapik et al., 2000), and in NGC 4414 (Soida et al., 2002). The mean degree of polarization (corrected for different spatial resolutions) is similar between grand-design and flocculent galaxies (Knapik et al., 2000).
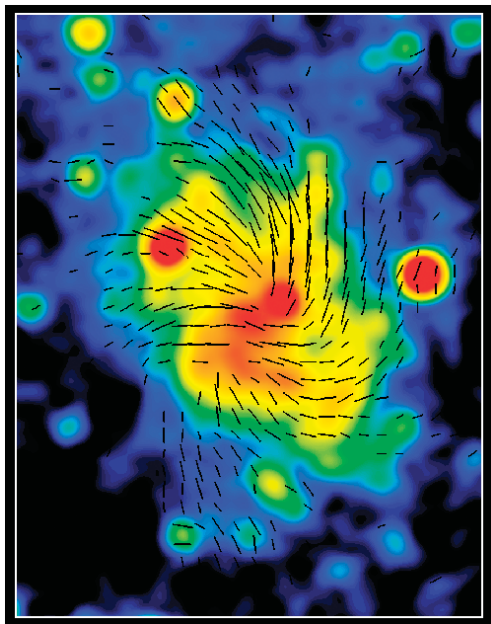
Fig. 15. Total radio emission (contours) and B–vectors of M 33 at λ6 cm, observed with the Effelsberg telescope. The field size is $51' \times 66'$, the beam size $3'$ (Niklas and Beck, unpublished)

Spiral patterns are observed in all flocculent galaxies, indicative that the dynamo works without assistance from density waves, as expected from the classical α–Ω dynamo. However, the multi-wavelength data of M 33 and NGC 4414 call for a mixture of modes or an even more complicated field structure (Fletcher et al., 2000; Soida et al., 2002).

Radio continuum maps of irregular, slowly rotating galaxies of the Local Group reveal strong total magnetic fields of more than $10\,\mu$G in the galaxies NGC 4449 (Fig. 16) and IC 10 (Chyży et al., 2003). Even dwarf irregular galaxies with almost chaotic rotation host total fields with strengths comparable to spiral galaxies if their star formation activity is sufficiently high so that the fluctuation dynamo (see
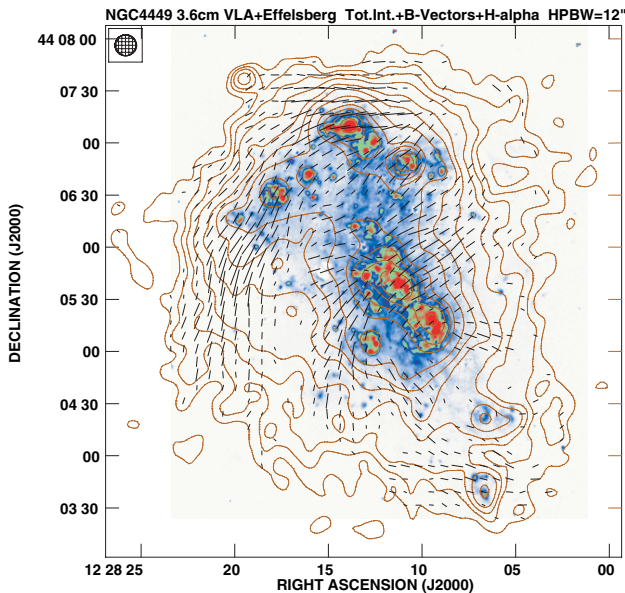
Fig. 16. Total radio emission (contours) and B–vectors of NGC 4449 at $\lambda 3.6$ cm with $12''$ beam size, combined from VLA and Effelsberg observations (Chyży et al., 2000). The background image shows the Hα emission

below) can operate. In these galaxies the energy density of the magnetic field is only slighly smaller than that of the (chaotic) rotation and thus may affect the evolution of the whole system. NGC 6822, on the other hand, has a low star-forming activity and only very weak total radio emission, i.e. a *total* field weaker than $5\,\mu$G, probably below the threshold for any type of dynamo action. As the production of cosmic rays is very low in NGC 6822, it is also possible that any existing magnetic field is not 'illuminated'.

In NGC 4449 (Fig. 16) the field is partly regular with some spiral pattern (Chyży et al., 2000), while in NGC 6822 the field is mostly tangled (Chyży et al., 2003). A few small spots of faint polarized emission indicate that the regular field in NGC 6822 is weaker than $5\,\mu$G, excluding the action of the classical α–Ω dynamo. Such galaxies require field amplification e.g. by the *fluctuation dynamo* (Kulsrud et al., 1997; Blackman, 1998; Subramanian, 1998; Schekochihin et al., 2004). Alternatively, some primordial field may have survived (Chap. 4), e.g. because velocity shear is smaller in irregular galaxies than in spiral galaxies.

The Magellanic Clouds are the closest irregular galaxies and deserve special attention. Polarization surveys with the Parkes telescope at several wavelengths revealed little polarized emission, only two magnetic filaments in the LMC south of the 30 Dor star-formation complex (Klein et al., 1998). The new ATCA polarization survey show that the LMC also hosts a large-scale magnetic field (Gaensler et al., 2005).

8 Magnetic Fields in Barred Galaxies

Gas and stars in strongly barred galaxies move in highly noncircular orbits. Numerical models show that gas streamlines are deflected in the bar region along shock

fronts, behind which the gas is compressed in a fast shearing flow (Athanassoula, 1992; Piner et al., 1995). As the gas in the bar region rotates faster than the bar, compression regions traced by massive dust lanes develop along the edge of the bar that is leading with respect to the galaxy's rotation. Gas inflow along the compression region may fuel starburst activity near the galactic center. Magnetic fields have not been included in the models.

M 83 is the nearest barred galaxy and shows compressed magnetic fields at both leading edges of the bar (Fig. 6).

The total and polarized radio continuum emission of 20 galaxies with large bars was observed with the Very Large Array (VLA) at λ3, 6, 18 and 22 cm and with the Australia Telescope Compact Array (ATCA) at λ6 cm and 13 cm (Beck et al., 2002, 2005). The total radio luminosity (measuring the total magnetic field) is strongest in galaxies with high far-infrared luminosity (indicating high star-formation activity), a result similar to that in non-barred galaxies. The average radio intensity, radio luminosity and star-formation activity all correlate with *relative bar length*.

Polarized emission was detected in 17 of the 20 barred galaxies. The pattern of the regular field in the galaxies with long bars (NGC 1097, 1365, 1559, 1672, 2442 and 7552) is significantly different from that in non-barred galaxies: Field enhancements occur outside of the bar (*upstream*), and the field lines are oriented at large angles with respect to the bar. The symmetry of the velocity fields in these galaxies is distorted by the bar's gravitational potential, leading to enhanced velocity shear, which may enhance dynamo action (Moss et al., 2001).

NGC 1097 (Fig. 17) hosts a huge bar of 16 kpc length. The total radio intensity (not shown in the figure) is strongest in the region of the dust lanes, consistent
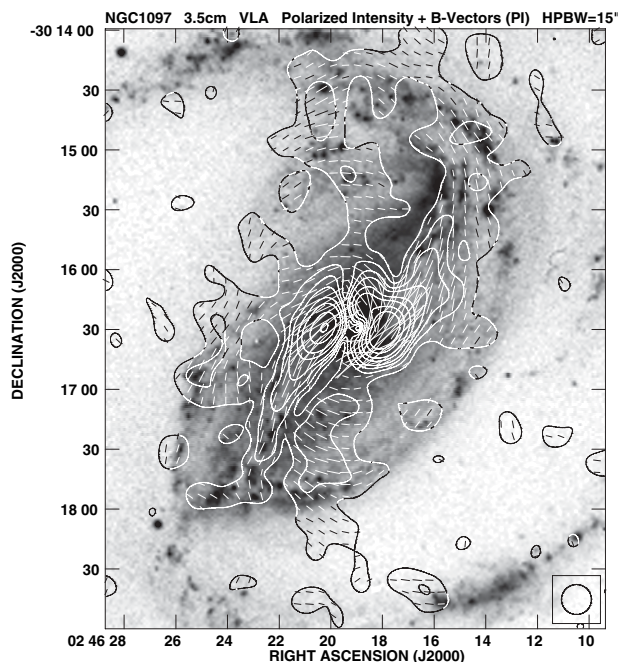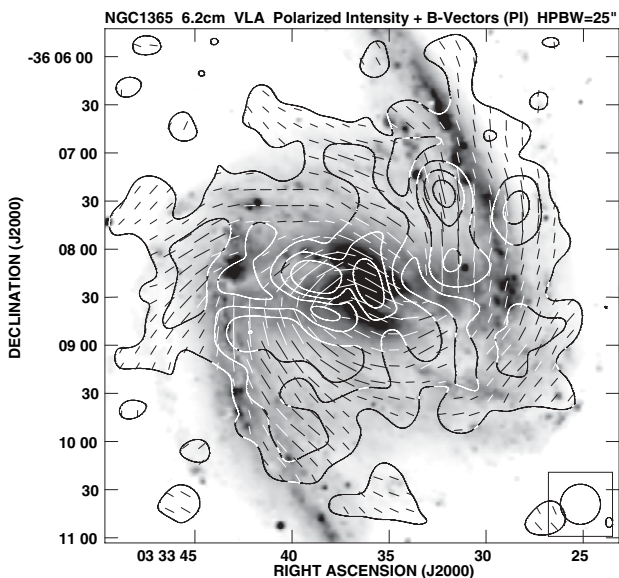

Fig. 17. Polarized radio emission (contours) and B–vectors of the barred galaxy NGC 1097 at λ3.5 cm with 15″ beam size, observed with the VLA (Beck et al., 1999a, 2005). The background optical image is from the Cerro Tololo Observatory (Arp, priv. comm.)

with compression by the bar's shock. The general similarity of the B–vectors in NGC 1097 and gas streamlines around the bar as obtained in numerical simulations (Athanassoula, 1992) is striking. This suggests that the regular magnetic field is aligned with the shearing flow (Beck et al., 1999a). In the southern bar, the upstream region (south of the center in in Fig. 17) and downstream region (southeast of the center, coinciding with the dust lanes) are separated in enhanced polarized emission by a strip of low polarized intensity where the regular field changes its orientation by almost $90°$. This observation implies that the region of strongest shear in the magnetic field is located $\simeq 800 \, \mathrm{pc}$ in front of the dust lanes, in contrast to the velocity field in the numerical simulations. Either the regular field is not coupled to the dense gas and avoids the shock, or the existing simulations are insufficient to model magnetized shocks. Remarkably, the optical image of NGC 1097 shows dust filaments in the upstream region which are almost perpendicular to the bar and thus aligned with the regular field.

NGC 1365 (Fig. 18) is similar to NGC 1097 in its overall properties, but the polarization data indicate that the magnetic shear due to the bar is weaker. The field bends even more smoothly from the upstream region into the bar, with no indication of a shock. NGC 1559, NGC 1672 and NGC 7552 show similar polarization features (Beck et al., 2002), but the spatial resolution is still insufficient to reveal the detailed structure of their regular fields.

The circumnuclear ring of NGC 1097 (Fig. 19) is a site of ongoing intense star formation, with an active nucleus in its centre. The orientation of the innermost spiral field agrees with that of the spiral dust filaments visible on optical images. Magnetic stress in the circumnuclear ring can drive mass inflow which is sufficient to fuel the activity of the nucleus (Beck et al., 1999a, 2005). Bright circumnuclear radio rings have also been found in the barred galaxies NGC 1672 and NGC 7552 (Beck et al., 2004).

Fig. 18. Polarized radio emission (contours) and B–vectors of NGC 1365 at $\lambda 6$ cm with $25''$ beam size, observed with the VLA (Beck et al., 2002, 2005). The background optical image is from the ESO (Lindblad, priv. comm.)

NGC1097-Center   3.5cm   VLA   Total Int. + B-Vectors (PI)   HPBW=3"
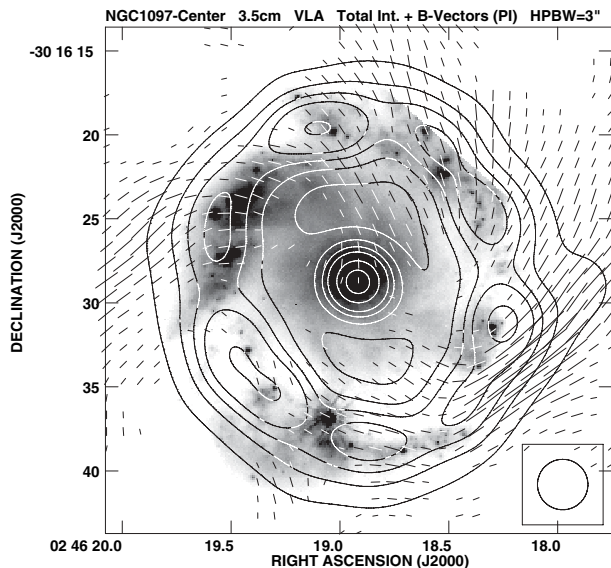
Fig. 19. Total radio emission (contours) and B–vectors from the central region of NGC 1097 at $\lambda 3.5$ cm with $3''$ beam size, observed with the VLA (Beck et al., 1999a, 2004). The background optical image is from the Hubble Space Telescope (Barth et al., 1995)

Radio polarization data have revealed a principal difference between the behaviours of magnetic fields in barred and non-barred galaxies. In non-barred galaxies the field lines are of overall spiral shape, they do not follow the gas flow and are probably controlled by dynamo action. In strongly barred galaxies the field mostly follows the gas flow, except in the upstream region where it (more or less) smoothly bends towards the bar. Polarized radio emission appears to be an excellent indicator of shearing motions.

9 Halos

Halo magnetic fields are important for the propagation of cosmic rays, the formation of a galactic wind and the stability of gas filaments. Their detection requires analysis of the Faraday effects on the polarized radio emission from the background disk of mildly inclined galaxies (e.g. in M 31, Fletcher et al., 2004a) or observation of edge-on galaxies.

The radio emission of most edge-on galaxies can be described by a thin disk plus a thick disk (halo), with similar scale heights of $\simeq 300$ pc for the thin and $\simeq 1.5$ kpc for the thick disk (Dumke and Krause, 1998; Dumke et al., 2000). The observed field orientations are mainly parallel to the disk (Dumke et al., 1995).

A prominent exception is NGC 4631 with the brightest and largest radio halo observed so far (Fig. 20), with a scale height of $\simeq 2.5$ kpc. In case of energy equipartition between magnetic fields and cosmic rays, the scale height of the total field is $\simeq 10$ kpc. The radio halo above the inner disk is composed of vertical magnetic spurs connected to star-forming regions in the disk (Golla and Hummel, 1994). The field is probably dragged out by a strong galactic wind. At larger radii where star formation is weaker, the field is parallel to the disk. Other galaxies with strong
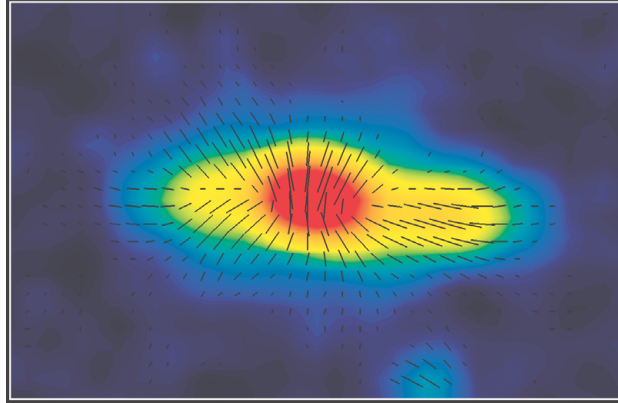
Fig. 20. Total radio emission (contours) and B–vectors of NGC 4631 at $\lambda 3.6$ cm, observed with the Effelsberg telescope. The field size is $17'$ x $11'$, the beam size $1.5'$ (Krause et al., in prep.)

winds are M 82 (Klein et al., 1998; Reuter et al., 1994) and NGC 4666 (Dahlem et al., 1997). Starburst-driven outflows can be the origin of intergalactic magnetic fields (Chap. 2).
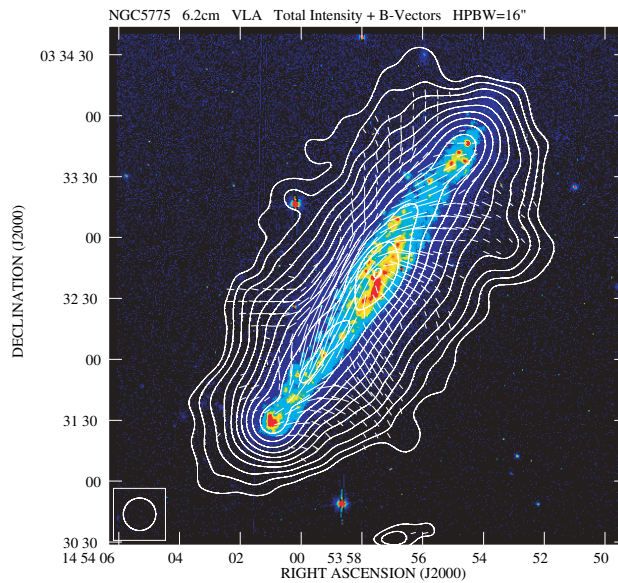
Fig. 21. Total radio emission (contours) and B–vectors of NGC 5775 at $\lambda 6$ cm with $16''$ beam size, observed with the VLA (Tüllmann et al., 2000)

NGC 5775 is an intermediate case with parallel and vertical field components (Fig. 21). The magnetic energy density in the halo of, e.g. M 83, exceeds that of the hot gas (Ehle et al., 1998), so that halo magnetic fields are important for the formation of a galactic wind. Magnetic reconnection is a possible heating source of the halo gas (Birk et al., 1998).

Dynamo models predict the preferred generation of quadrupole fields where the toroidal component has the same sign above and below the plane, as claimed for the

Milky Way (Han et al., 1997). In external galaxies the vertical field symmetry could not yet been determined with sufficient accuracy. Indirect evidence for preferred quadrupole-type fields follows from the possible dominance of inward-directed radial field components (Krause and Beck, 1998). The dominance of one direction is in conflict with dipolar fields where the toroidal field reverses in the plane, so that the observed field direction depends on the aspect angle and no preference is expected for a galaxy sample. (Note that Faraday rotation is *not* zero along a line of sight passing through a disk containing a field reversal if cosmic-ray and thermal electrons are mixed in the disk. The sign of Faraday rotation traces the field direction in the layer which is *nearer* to the observer.)

10 Interacting Galaxies

Violently disrupted galaxies show strong departures from symmetric gas flows. Magnetic fields trace regions of gas compression, strong shear and enhanced turbulence.

The classical interacting galaxy pair is NGC 4038/39, the 'Antennae' (Fig. 22), with bright, extended radio emission filling the body of the whole system, with no dominant nuclear sources. Particularly strong emission comes from a star-forming region, hidden in dust, at the southern end of a massive cloud complex extending between the galaxies (the dark extended region in Fig. 22). In this region, highly tangled magnetic fields reach strengths of $\simeq 30\,\mu$G, much larger than in both individual galaxies, probably the result of compression of original fields pulled out from the parent disks. Away from star-forming regions the magnetic field shows a coherent polarized structure with a strong regular component of $10\,\mu$G, probably the result of gas shearing motions along the tidal tail. The mean total magnetic fields in both galaxies are about two times stronger than in normal spirals, but
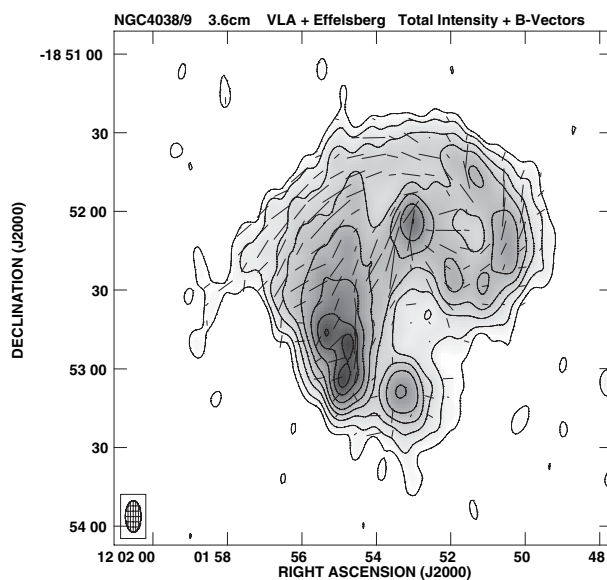
Fig. 22. Total radio emission (contours) and B–vectors of the 'Antennae' galaxy pair NGC 4038/39 at $\lambda 3.6$ cm with $6''$ x $12''$ beam size, combined from VLA and Effelsberg observations (Chyży and Beck, 2004)

the degree of field regularity is unusually low, implying destruction of the regular component in regions with strong star formation due to the interaction.

Interaction with a dense intergalactic medium also imprints unique signatures onto magnetic fields and thus the radio emission. Tidal interactions within the Leo Triplet is the probable cause of the asymmetric appearance of NGC 3627. While the regular field in the western half is strong and precisely follows the dust lanes, a bright *magnetic arm* in the eastern half crosses the optical arm and its massive dust lane at a large angle (Fig. 13). No counterpart of this feature was detected in any other spectral range. Either the optical arms has been recently deformed due to interaction or ram pressure, or the magnetic arm is an out-of-plane feature generated by interaction.

Ram pressure of the intergalactic medium compresses the magnetic field, so that strong polarized emission is observed on one side of the galaxy, as e.g. in NGC 2276 (Hummel and Beck, 1995). The massive northern spiral arm of NGC 2442 with the polarized emission shifted towards the outer edge (Fig. 12) is also a result of ram pressure.

The Virgo cluster is a location of especially strong interaction effects. The magnetic field is of NGC 4522 is strongly compressed at the eastern side of the galaxy (Fig. 23). This kind of behaviour is also observed in another Virgo spiral galaxy, NGC 4254 (Soida et al., 1996), and might be sign of ram pressure by the intracluster medium (ICM).

Interaction may also induce violent star-formation activity in the nuclear region or in the disk which may produce huge radio lobes due to outflowing gas and magnetic field. The lobes of the Virgo spiral NGC 4569 reach out to 24 kpc from the disk and are highly polarized (Fig. 24). However, there is neither an active nucleus nor a recent starburst in the disk, so that the radio lobes probably are a signature of activity in the past.
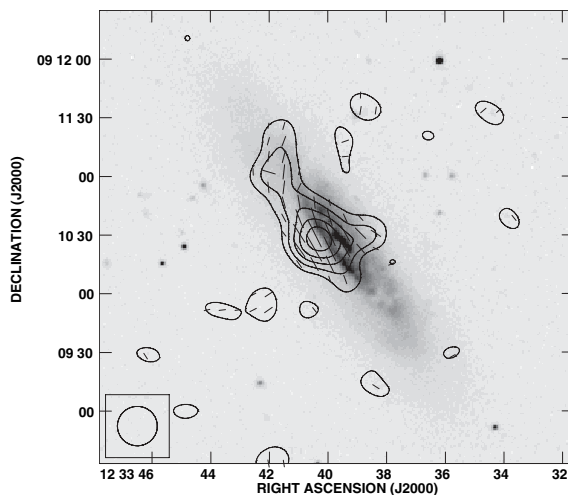
Fig. 23. Polarized radio emission (contours) and B–vectors of the Virgo galaxy NGC 4522 at $\lambda 6\,\mathrm{cm}$ with $20''$ beam size, observed with the VLA (Vollmer et al., 2004)
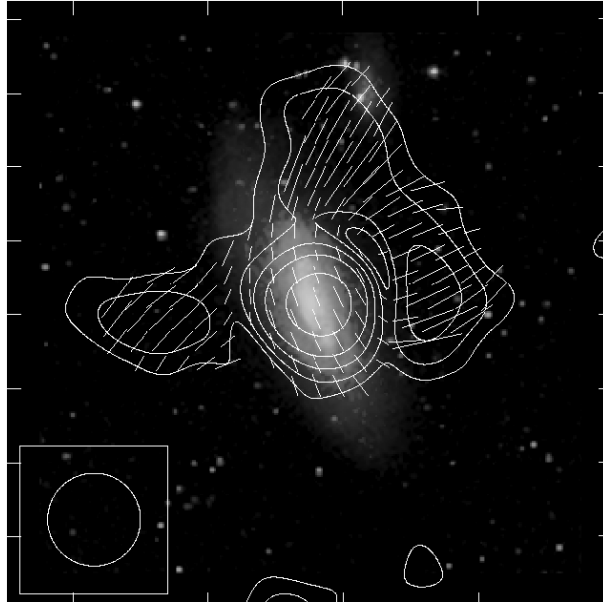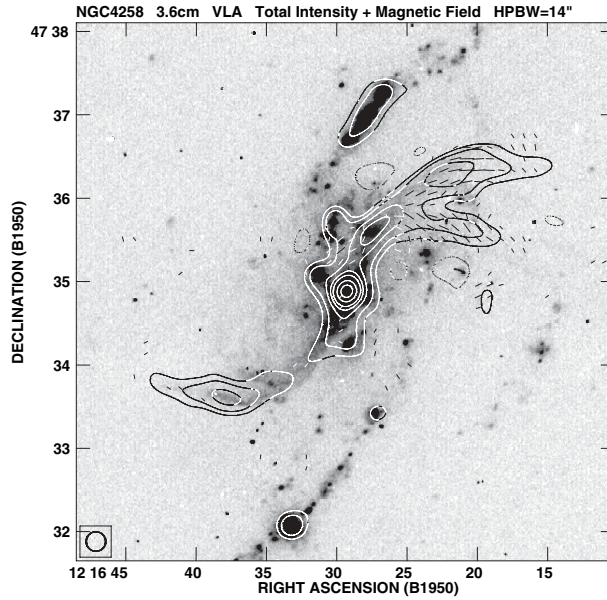
Fig. 24. Polarized radio emission (contours) and B–vectors of NGC 4569 at λ6.2 cm with $2.5'$ beam size, observed with the Effelsberg telescope (Chyży et al., in prep)

11 Spiral Galaxies with Jets

Many (maybe most) spiral galaxies host nuclear jets. These are weak and small compared to those of radio galaxies and quasars. Detection is further hampered by the fact that they emerge at some angle with respect to the disk, so that little interaction with the ISM occurs. Only if the accretion disk is oriented almost perpendicular to the disk, the jet hits a significant amount of ISM matter. Such a geometry was first proven for NGC 4258 by observations of the water maser emission from the accretion disk (Greenhill et al., 1995). This is why NGC 4258 is one of the rare cases where a large-scale radio jet can be observed (van Albada and van der Hulst, 1982; Krause and Löhr, 2004).

The total intensity map of NGC 4258 (Fig. 25) reveals that the jets emerge from the galactic centre perpendicular to the accretion disk, which is oriented in east-west direction and is seen almost edge-on, and bend out to become the 'anomalous radio arms' visible out to the boundaries of the spiral galaxy. The magnetic field orientation is mainly along the jet direction. The observed tilt with respect to the jet axis may indicate an additional toroidal field component or a helical field around the jet. The equipartition strength is about $300\,\mu$G for a relativistic electron-proton jet and $\simeq 100\,\mu$G for a relativistic electron-positron jet. Two parallel CO ridges on both sides along the jets in NGC 4258 indicate a tunnel with walls made of molecular gas, filled with hot ionized gas that is entrained by the jet travelling along the axis of the tunnel (Krause et al., in prep.).

Highly polarized radio emission from kpc-sized jets has also been detected e.g. in NGC 3079 (Cecil et al., 2001), in the barred galaxy NGC 7479 (Fig. 26, with the field orientations perpendicular to the jet's axis), and in the outflow lobes of the Circinus Galaxy (Elmouttie et al., 1995).

NGC4258   3.6cm   VLA   Total Intensity + Magnetic Field   HPBW=14"

Fig. 25. Total radio emission (contours) and B–vectors (corrected for Faraday rotation) of NGC 4258 at $\lambda 3.6$ cm with $14''$ beam size, observed with the VLA (Krause and Löhr, 2004). The background image shows an Hα image taken at the Hoher List Observatory of the University of Bonn

NGC7479   2.8cm   Effelsberg   Polarized Int. + B-Vectors   HPBW=69"
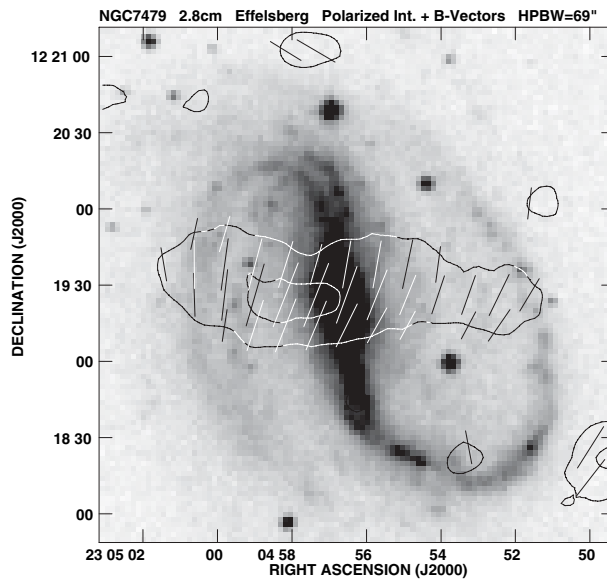
Fig. 26. Polarized radio emission (contours) and B–vectors of NGC 7479 at $\lambda 2.8$ cm with $69''$ beam size, observed with the Effelsberg telescope (Beck and Shoutenkov, unpublished)

12 Outlook

Thanks to radio polarization observations of external galaxies, much has been learnt about the global properties of interstellar magnetic fields, complemented by polarization observations in our Galaxy (Chap. 5) which trace structures of pc and sub-pc sizes. However, the physical connection between the features at large and

small scales is not understood. Radio observations of external galaxies at better resolution are needed to see the full wealth of magnetic structures in galaxies.

In future, new polarimeters in front of bolometer arrays (Siringo et al., 2004) will allow observations of external galaxies in the submm range with unprecedented sensitivity.

In radio continuum, the EVLA will soon allow radio polarization observations with increased sensitivity and resolution. A much larger step is planned for the next decade. The Square Kilometer Array (SKA) will be able to map nearby galaxies with at least 10x better angular resolution compared to present-day radio telescopes, or 10x more distant galaxies with similar spatial resolution as today (Beck and Gaensler, 2004). Magnetic field structures will illuminate the dynamical interplay of cosmic forces, such as loops, twisted fibres and field reversals, which are of 0.1–10 pc width. Polarimetry of reconnection regions would help to understand the heating of the interstellar gas. Imaging of field loops with helical twist would clarify how the dynamo operates. With a field strength of 30 μG and 1 pc extent along the line of sight, a (distance-independent) polarization surface brightness of 0.2 μJy per arcsec beam at 5 GHz is expected. The SKA will detect such features in the Magellanic Clouds (0.24 pc/arcsec) and in M 31 and M 33 (3.5 pc/arcsec).

The SKA's sensitivity will even allow to detect synchrotron emission from the most distant galaxies in the earliest stage of evolution and to search for the earliest magnetic fields and their origin.

References

van Albada, G. D., van der Hulst, J. M.: 1982, A&A 115, 263 43, 63

de Avillez, M., Breitschwerdt, D.: 2004, Ap&SS 292, 207 41

Appenzeller, I.: 1967, PASP 79, 600 42

Athanassoula, E.: 1992, MNRAS 259, 345 57, 58

Barth, A. J., Ho, L. C., Filippenko, A. V., Sargent, W. L. W.: 1995, AJ 110, 1009 59

Battaner, E., Florido, E.: 2000, Fund. Cosmic Phys. 21, 1 45

Beck, R.: 1982, A&A 106, 121

Beck, R.: 1993, In: *The Cosmic Dynamo*, ed. F. Krause et al. (Dordrecht: Kluwer), p. 283

Beck, R.: 2000, Phil. Trans. R. Soc. Lond. A 358, 777 42, 53

Beck, R.: 2001, Sp. Sci. Rev. 99, 243 53

Beck, R.: 2004, In: *How Does the Galaxy Work?*, ed. E. J. Alfaro et al. (Dordrecht: Kluwer), p. 277 45

Beck, R., Hoernes, P.: 1996, Nat 379, 47 50

Beck, R., Gaensler, B. M.: 2004, In: *Science with the Square Kilometer Array*, ed. C. Carilli & S. Rawlings (Amsterdam: Elsevier), New Astronomy Reviews 48, 1289, astro-ph/0409368 55, 65

Beck, R., Krause, M.: 2005, AN 326, 414 44

Beck, R., Berkhuijsen, E. M., Wielebinski, R.: 1978, A&A 68, L27 42

Beck, R., Berkhuijsen, E. M., Wielebinski, R.: 1980, Nat 283, 272 42

Beck, R., Brandenburg, A., Moss, D., Shukurov, A., Sokoloff, D.: 1996, ARA&A 34, 155 41, 53

Beck, R., Ehle, M., Shoutenkov, V., Shukurov, A., Sokoloff, D.: 1999a, Nat 397, 324 57, 58, 59

Beck, R., Berkhuijsen, E. M., Uyanıker, B.: 1999b, In: *Plasma Turbulence and Energetic Particles in Astrophysics*, ed. M. Ostrowski & R. Schlickeiser, Kraków, p. 5 53

Beck, R., Shoutenkov, V., Ehle, M., et al.: 2002, A&A 391, 83 57, 58

Beck, R., Shukurov, A., Sokoloff, D., Wielebinski, R.: 2003, A&A 411, 99 44

Beck, R., Ehle, M., Fletcher, A., et al.: 2004, in: *The Evolution of Starbursts*, ed. S. Hüttemeister et al., AIP Conf. Proc., in press 44, 58, 59

Beck, R., Fletcher, A., Shukurov, A., et al.: 2005, A&A, submitted 57, 58

Belyanin, M., Sokoloff, D., Shukurov, A.: 1993, Geophys. Astrophys. Fluid Dyn. 68, 227

Berkhuijsen, E. M., Horellou, C., Krause, M., et al.: 1997, A&A 318, 700 53

Berkhuijsen, E. M., Beck, R., Hoernes, P.: 2003, A&A 398, 937 48, 54

Birk, G. T., Lesch, H., Neukirch, T.: 1998, MNRAS 296, 165 41, 60

Blackman, E. G.: 1998, ApJ 496, L17 56

Boulares, A., Cox, D. P.: 1990, ApJ 365, 544 44, 45

Brandenburg, A., Urpin, V.: 1998, A&A 332, L41 54

Buczilowski, U. R., Beck, R.: 1991, A&A 241, 47

Cecil, G., Bland-Hawthorn, J., Veilleux, S., Filippenko, A. V.: 2001, ApJ 555, 338 63

Chyży, K. T., Beck, R.: 2004, A&A 417, 541 61

Chyży, K. T., Beck, R., Kohle, S., et al.: 2000, A&A 356, 757 56

Chyży, K. T., Knapik, J., Bomans, D. J., et al.: 2003, A&A 405, 513 55, 56

Crutcher, R.M.: 1999, ApJ 520, 706

Dahlem, M., Petr, M. G., Lehnert, M. D., et al.: 1997, A&A 320, 731 60

Dumke, M., Krause, M.: 1998, In: *The Local Bubble and Beyond*, ed. D. Breitschwerdt et al. (Berlin: Springer), p. 555 59

Dumke, M., Krause, M., Wielebinski, R., Klein, U.: 1995, A&A 302, 691 59

Dumke, M., Krause, M., Wielebinski, R.: 2000, A&A 355, 512 59

Ehle, M., Beck, R., Haynes, R. F., et al.: 1996, A&A 306, 73 43, 49

Ehle, M., Pietsch, W., Beck, R., Klein, U.: 1998, A&A 329, 39 45, 60

Elmegreen, B.G.: 1981, ApJ 243, 512 41

Elmouttie, M., Haynes, R. F., Jones, K. L., et al.: 1995, MNRAS 275, L53 63

Elstner, D., Otmianowska-Mazur, K., von Linden, S., Urbanik, M.: 2000, A&A 357, 129 53

Fan, Z., Lou, Y.-Q.: 1997, MNRAS 291, 91 51

Fendt, Ch., Beck, R., Neininger, N.: 1998, A&A 335, 123 42

Ferguson, A. M. N., Wyse, R. F. G., Gallagher, J. S., Hunter, D. A.: 1998, ApJ 506, L19 50

Fletcher, A., Beck, R., Berkhuijsen, E. M., Shukurov, A.: 2000, In: *The Interstellar Medium in M 31 and M 33*, ed. E. M. Berkhuijsen et al. (Aachen: Shaker), p. 201 55

Fletcher, A., Berkhuijsen, E. M., Beck, R., Shukurov, A.: 2004a, A&A 414, 53 54, 59

Fletcher, A., Beck, R., Berkhuijsen, E. M., Horellou, C., Shukurov, A.: 2004b, In: *How Does the Galaxy Work?*, ed. E. J. Alfaro et al. (Dordrecht: Kluwer), p. 299 44, 46, 47

Frick, P., Beck, R., Berkhuijsen, E.M., Patrickeyev, I.: 2001, MNRAS 327, 1145 45

Gaensler, B. M., Haverkorn, M., Staveley-Smith, L., et al.: 2005, Science 307, 1610 53, 56

Golla, G., Hummel, E.: 1994, A&A 284, 777 59

Gómez, G. C., Cox, D. P.: 2002, ApJ 580, 235 41, 49

Greaves, J. S., Murray, A. G., Holland, W. S.: 1994, A&A 284, L19 47

Greaves, J. S., Holland, W. S., Jenness, T., Hawarden, T. G.: 2000, Nat 404, 732 42

Greenhill, L. J., Jiang, D. R., Moran, J. M., et al.: 1995, ApJ 440, 619 63

Han, J. L., Manchester, R. N., Berkhuijsen, E. M., Beck, R.: 1997, A&A 322, 98 45, 61

Han, J.L., Beck, R., Berkhuijsen, E.M.: 1998, A&A 335, 1117 49, 54

Han, J. L., Beck, R., Ehle, M., Haynes, R. F., Wielebinski, R.: 1999, A&A 348, 405 49, 51, 53, 54

Hanasz, M., Lesch, H.: 2000, ApJ 543, 235 54

Hanasz, M., Otmianowska-Mazur, K., Lesch, H.: 2002, A&A 386, 347 54

Harnett, J., Ehle, M., Fletcher, A., et al.: 2004, A&A 421, 571 51, 52

Hildebrand, R. H.: 1988, QJRAS 29, 327 42

Hiltner, W. A.: 1958, ApJ 128, 9 42

Hoernes, P.: 1997, PhD thesis, University of Bonn 53

Hoernes, P., Berkhuijsen, E. M., Xu, C.: 1998, A&A 334, 57 46

Hummel, E., Beck, R.: 1995, A&A 303, 691 62

Klein, U., Wielebinski, R., Morsi, H. W.: 1988, A&A 190, 41 44, 56, 60

Klein, U., Haynes, R. F., Wielebinski, R., Meinert, D.: 1993, A&A 271, 402

Knapik, J., Soida, M., Dettmar, R.-J., et al.: 2000, A&A 362, 910 55

Krause, F., Beck, R.: 1998, A&A 335, 789 61

Krause, M.: 1990, In: *Galactic and Intergalactic Magnetic Fields*, ed. R. Beck et al. (Dordrecht: Kluwer), p. 187

Krause, M.: 1993, In: *The Cosmic Dynamo*, ed. F. Krause et al. (Dordrecht: Kluwer), p. 305 52

Krause, M., Löhr, A.: 2004, A&A 420, 115 63, 64

Krause, M., Hummel, E., Beck, R.: 1989a, A&A 217, 4 52

Krause, M., Beck, R., Hummel, E.: 1989b, A&A 217, 17 49, 52, 54

Kulsrud, R. M., Cen, R., Ostriker, J. P., Ryu, D.: 1997, ApJ 480, 481 56

von Linden, S., Otmianowska-Mazur, K., Lesch, H., Skupniewicz, G.: 1998, A&A 333, 79 53

Mathewson, D. S., van der Kruit, P. C., Brouw, W. N.: 1972, A&A 17, 468 42

Mestel, L.: 1990, In: *Galactic and Intergalactic Magnetic Fields*, ed. R. Beck et al. (Dordrecht: Kluwer), p. 259 41

Mitra, D., Wielebinski, R., Kramer, M., Jessner, A.: 2003, A&A 398, 993 53

Moss, D.: 1998, MNRAS 297, 860

Moss, D., Shukurov, A., Sokoloff, D.: 1999, A&A 343, 120 54

Moss, D., Shukurov, A., Sokoloff, D., Beck, R., Fletcher, A.: 2001, A&A 380, 55 57

Mouschovias, T. Ch.: 1990, In: *Galactic and Intergalactic Magnetic Fields*, ed. R. Beck et al. (Dordrecht: Kluwer), p. 269 41

Neininger, N.: 1992, A&A 263, 30

Neininger, N., Horellou, C.: 1996, In: *Polarimetry of the Interstellar Medium*, ed. W. G. Roberge & D. C. B. Whittet, ASP Conf. Ser. 97, p. 592

Neininger, N., Klein, U., Beck, R., Wielebinski, R.: 1991, Nat 352, 781

Niklas, S.: 1995, PhD thesis, University of Bonn 44

Niklas, S., Beck, R.: 1997, A&A 320, 54 46

Parker, E. N.: 1992, ApJ 401, 137 54

Piner, B. G., Stone, J. M., Teuben, P. J.: 1995, ApJ 449, 508 57

Priklonsky, V.I., Shukurov, A., Sokoloff, D., Soward, A.: 2000, Geophys. Astrophys. Fluid Dyn. 93, 97

Reuter, H.-P., Klein, U., Lesch, H., et al.: 1994, A&A 282, 724 60

Rohde, R., Beck, R., Elstner, D.: 1999, A&A 350, 423 54

Rüdiger, G., Hollerbach, R.: 2004, *The Magnetic Universe* (Weinheim: Wiley-VCH), p. 261 45, 54

Sauvage, M., Blommaert, J., Boulanger, F., et al.: 1996, A&A 315, L89 45, 46

Scarrott, S. M., White, C., Pallister, W. S., Solinger, A. B.: 1977, Nat 265, 32 42

Scarrott, S. M., Ward-Thompson, D., Warren-Smith, R. F.: 1987, MNRAS 224, 299

Schekochihin, A. A., Cowley, S. C., Taylor, S. F., et al.: 2004, ApJ 612, 276 56

Schoofs, S.: 1992, Diploma thesis, University of Bonn 49

Sellwood, J. A., Balbus, S. A.: 1999, ApJ 511, 660 45, 54

Shukurov, A.: 1998, MNRAS 299, L21

Siringo, G., Kreysa, E., Reichertz, L. A., Menten, K. M.: 2004, In: *The Magnetized Interstellar Medium*, ed. B. Uyanıker et al. (Katlenburg-Lindau: Copernicus), p. 215 65

Soida, M., Urbanik, M., Beck, R.: 1996, A&A 312, 409 52, 62

Soida, M., Urbanik, M., Beck, R., Wielebinski, R., Balkowski, C.: 2001, A&A 378, 40 52

Soida, M., Beck, R., Urbanik, M., Braine, J.: 2002, A&A 394, 47 53, 55

Sokoloff, D. D., Bykov, A. A., Shukurov, A., et al.: 1998, MNRAS 299, 189, and MNRAS 303, 207 (Erratum) 43, 48

Stacey, G. J., Geis, N., Genzel, R., et al.: 1991, ApJ 373, 423 46

Strong, A. W., Moskalenko, I. V., Reimer, O.: 2000, ApJ 537, 763 44

Subramanian, K.: 1998, MNRAS 294, 718 41, 56

Tüllmann, R., Dettmar, R.J., Soida, M., Urbanik, M., Rossa, J.: 2000, A&A 364, L36 60

Vollmer, B., Beck, R., Kenney, J. D. P., van Gorkum, J. H.: 2004, AJ 127, 3375 62

Walsh, W., Beck, R., Thuma, G., et al.: 2002, A&A 388, 7 45

Wielebinski, R., Krause, F.: 1993, A&AR 4, 449 41

Wolleben, M., Reich, W.: 2004, A&A 427, 537 47